Vipin Kumar Marina L. Gavrilova
Chih Jeng Kenneth Tan Pierre L'Ecuyer (Eds.)

# Computational Science and Its Applications – ICCSA 2003

International Conference
Montreal, Canada, May 18-21, 2003
Proceedings, Part II

Springer

cs front tracking code; A
3985, Los Alamos National

hang. Quantitative theory
l):3473–3476, 1993.
ion of a shock wave at a

nvestigation of Richtmyer-
301:51–64, 1995.
tmyer-Meshkov instability
998.

# Computational Aspects of Conservative Difference Schemes for Shape Memory Alloys Applications

R.V.N. Melnik[1], L. Wang[1], P. Matus[2], and I. Rybak[2]

[1] University of Southern Denmark,
Mads Clausen Institute, DK-6400, Denmark
[2] Institute of Mathematics, National Academy of
Sciences, Minsk, 220072, Belarus

**Abstract.** In this paper we describe a new conservative difference scheme and apply it to the description of the dynamics of a shape memory alloy rod. The scheme preserves the conservation of the total energy on the grid. A major emphasis is given to the description of hysteresis effects in almost-elastic, pseudoelastic and quasiplastic regimes. Stress-strain dependencies are analysed and computational experiments are presented for main thermomechanical characteristics of the material, including displacement and temperature fields.

## 1 Introduction

Due to a wide range of existing and potential applications, the dynamics of smart materials has intensively been studied by experimentalists. In particular, it is known that such metallic alloys as NiTi, NiAl, CuZnGa, CuZnAl, CuZn, CuAlNi, AuCuZn exhibit a hysteretic behavior and shape memory effects, subject to adequate thermomechanical conditions. Hysteresis effects are often accompanied by phase transformations which are intrinsic to such materials and which occur with a shearing motion of the crystal atoms. Since no large movements of atoms are required to achieve such transformations they are often termed as "diffusionless", reflecting the fact that they occur practically instantaneously. To describe such transformations and to quantify accompanied them hysteresis effects is a challenging computational task.

As a starting point of our present discussion we choose the Landau-Ginzburg-Devonshire model for the free energy function, assuming that any isothermal equilibrium configuration of the lattice corresponds to a minimum (either local or global) of that function. Since the shape memory material can be in a high temperature phase (austenite) as well as in a low temperature phase (martensite), at the computational level one faces a fairly complex task of dealing with different equilibrium configurations of the metallic lattice simultaneously.

A better understanding of the dynamics of shape memory materials is important for many areas applications. These materials are an intrinsic part of the smart material and structure technology. They can directly transduce thermal

V. Kumar et al. (Eds.): ICCSA 2003, LNCS 2668, pp. 791–800, 2003.

energy into mechanical and vice versa, making them very attractive in microsensor and actuator applications. Other application areas include biomedicine, communication industries, robotics to name just a few. The analysis of shape memory materials has attracted a considerable attention of researchers, both experimentalists and theorists (e.g., [1,2,3,4,5,6,7]). Computational aspects of modelling shape memory materials have also been in the focus of a number of papers. One of the first papers in this field was [3] where the authors constructed and analysed a finite element approximation to a system describing phase transformations in a simple one-dimensional shape memory sample. In a series of papers [4,5,8] the authors developed a generic procedure based on a low-dimensional reduction of the general three-dimensional systems describing the dynamics of shape memory materials. While at a theoretical level the authors used effectively a blend between the centre manifold technique and computer algebra, the underlying numerical implementation was based on a differential-algebraic solver. However, except of the recent paper [9], there has been no a systematic discussion in the literature devoted to fully conservative difference schemes for shape memory material applications. The construction of such schemes is a difficult task due to a strong nonlinear coupling of the associated system of partial differential equations. In this paper, we describe a new conservative scheme and present, for the first time, numerical results obtained with this scheme.

## 2 The Model for Shape Memory Material Dynamics

In what follows, we employ the Helmholtz free energy function

$$\psi(\theta, \epsilon) = \psi_0(\theta) + \psi_1(\theta)\psi_2(\epsilon) + \psi_3(\epsilon) \tag{1}$$

that satisfies all requirements of the Landau theory of structural phase transitions and is capable of describing phase transformations in materials with shape memory effects (e.g., [2]). In (1) by $\theta$ we denote the temperature field, and by $\epsilon$ we denote the macroscopic strain in the system which implicitly takes into account microscopic deformations of the crystal lattice. The terms $\psi_0$ and $\psi_3$ in (1) model contributions of the thermal field and the mechanical field, respectively, while the product $\psi_1\psi_2$ models shape-memory contributions. All these terms are taken in the Landau-Ginzburg-Devonshire form. Within this framework, the governing equations for the dynamics of a one-dimensional shape memory alloy rod can be written as the following coupled system of nonlinear equations with quintic order of nonlinearities in strain

$$\begin{aligned} \rho\frac{\partial^2 u}{\partial t^2} &= \frac{\partial}{\partial x}\left(k_1(\theta-\theta_1)\frac{\partial u}{\partial x} - k_2\left(\frac{\partial u}{\partial x}\right)^3 + k_3\left(\frac{\partial u}{\partial x}\right)^5\right) + F, \\ C_v\frac{\partial \theta}{\partial t} &= k\frac{\partial^2 \theta}{\partial x^2} + k_1\theta\frac{\partial u}{\partial x}\frac{\partial v}{\partial x} + G. \end{aligned} \tag{2}$$

In (2) $u$ is the displacement of the rod, $\rho$ is the density of the material, $k$ is the thermal conductivity of the material, $C_v$ is the specific heat constant of

the material, $\theta_1$ is a positive constant that characterises a critical temperature of the material, $k_1$, $k_2$ and $k_3$ are material-specific constants that characterise the material free energy, and $F$ and $G$ are distributed mechanical and thermal loadings.

System (2) is completed by appropriate initial and boundary conditions and has to be solved with respect to $(u, \theta)$ in the spatial-temporal region $\Omega = \{(x,t) : 0 \le x \le L, 0 \le t \le T_f\}$, where $L$ is the length of the shape memory rod and $T_f$ is the limiting time moment. The initial conditions for the system (2) are taken in the following form

$$u(x,0) = u^0(x), \qquad v(x,0) = \frac{\partial u}{\partial t}(x,0) = u^1(x), \qquad \theta(x,0) = \theta^0(x), \tag{3}$$

with specified functions $u^0$ , $u^1$ , $\theta^0$. Boundary conditions are problem-specific. In all computational experiments reported in this paper, mechanical boundary conditions are specified by stress:

$$s(0,t) = \bar{s}_1(t), \qquad s(L,t) = \bar{s}_2(t), \tag{4}$$

where $\bar{s}_1(t)$ and $\bar{s}_2(t)$ are given functions of time. Thermal boundary conditions are those of the specified heat flux

$$\frac{\partial \theta}{\partial x}(0,t) = \bar{\theta}_1(t), \qquad \frac{\partial \theta}{\partial x}(L,t) = \bar{\theta}_2(t), \tag{5}$$

where functions $\bar{\theta}_1(t)$ and $\bar{\theta}_2(t)$ are given. The governing equations (2) together with initial conditions (3) and boundary conditions (4), (5) will be used here as the basic model for our computational analysis of nonlinear dynamics of shape memory materials.

## 3 Conservative Scheme for the Analysis of Shape Memory Effects

The success of modelling is often dependent on how well the invariant properties of the original differential model are reflected in the numerical approximation. Efficient procedures for constructing such numerical schemes that preserve characteristic properties (in particular, those expressed by conservation laws) of the original model are well developed for linear problems (e.g., [10]). An efficient methodology that generalised the existing linear theory to several classes of non-linear PDE models was proposed in [11]. Recently, a conservative difference scheme has been proposed for the Cahn-Hilliard equation describing a phase separation phenomenon [12]. The idea employed in this paper for the construction of fully conservative schemes is based on the integro-interpolational methodology with the following modification. In addition to the interpolation of the sought-for solution with respect to independent variables, we also need to perform the Steklov averaging of nonlinear terms.

One of the difficulties in the numerical solution of system (3)–(5) lies with the fact that the stress-strain dependency here is a non-monotone function. In [4,5,8] an efficient numerical methodology was developed based on a reduction of the original model to a system of differential-algebraic equations. The main differential variables of the system were $u$, $v$, and $\theta$, while the equation for stress was handled as a differential-algebraic equation. In what follows, a different idea is developed. We will treat the stress-strain dependency as a purely algebraic equation by introducing $\epsilon$, $v$, and $\theta$ as differential variables, in which case $s$ can be written as an algebraic equation in terms of $\epsilon$

$$\begin{aligned} &\epsilon = \frac{\partial u}{\partial x}, \quad v = \frac{\partial u}{\partial t}, \\ &s = k_1(\theta - \theta_1)\epsilon - k_2\epsilon^3 + k_3\epsilon^5. \end{aligned} \tag{6}$$

Taking into account (6), problem (2)–(5) can be recast into the following form:

$$\begin{aligned} &\frac{\partial \epsilon}{\partial t} = \frac{\partial v}{\partial x}, \\ &\rho\frac{\partial v}{\partial t} = \frac{\partial s}{\partial x} + F, \\ &C_v\frac{\partial \theta}{\partial t} = k\frac{\partial^2 \theta}{\partial^2 x} + k_1\theta\epsilon\frac{\partial v}{\partial x} + G, \\ &s = k_1(\theta - \theta_1)\epsilon - k_2\epsilon^3 + k_3\epsilon^5, \\ &\epsilon(x,0) = \frac{\partial u^0(x)}{\partial x}, \quad v(x,0) = u^1(x), \quad \theta(x,0) = \theta^0(x), \\ &s(0,t) = \bar{s}_1(t), \quad s(L,t) = \bar{s}_2(t), \quad \frac{\partial \theta}{\partial x}(0,t) = \bar{\theta}_1(t), \quad \frac{\partial \theta}{\partial x}(L,t) = \bar{\theta}_2(t), \end{aligned} \tag{7}$$

In [9] it has recently been shown that in the absence of distributed loadings systems like (7) are characterised by the conservation law of the total energy which can be written in the following form

$$\mathcal{E}(t) = \mathcal{E}(0), \tag{8}$$

where the full energy of the system is understood as

$$\mathcal{E}(t) = \rho\|v\|^2 + (2C_v\theta - k_1\theta_1\epsilon^2 - \frac{k_2}{2}\epsilon^4 + \frac{k_3}{3}\epsilon^6, 1) - \int_0^t (2k\frac{\partial \theta}{\partial x} + sv)|_0^t dt \tag{9}$$

with scalar products taken in space $L_2$. The property (8)–(9) can be preserved on the grid if we follow the methodology described below.

In the closed interval $[0, L]$, we define the space grid with integer points $x_i$ and flux points $\bar{x}_i$ as follows,

$$x_i = ih, i = 0, 1, 2, \cdots, N, \qquad \bar{x}_i = (i + \frac{1}{2})h, i = 0, 1, 2, \cdots, N-1,$$

where $N$ is the number of grid points satisfying equality $hN = L$. Strain $\epsilon$, temperature $\theta$ and stress $s$ are approximated in the integer grid points $x_i$ and are denoted here by $\epsilon_i$, $\theta_i$ and $s_i$, respectively, while velocity $v$ is approximated in the flux points $\bar{x}_i$ and is denoted here by $v_i$. We note that the scheme described below is a second order scheme obtained on the minimal stencil [9]. Nonlinear terms (in particular, $\epsilon^4$ and $\epsilon^6$) are averaged here in the Steklov sense, so that for nonlinear function $f(\xi)$, averaged in the the interval $[\epsilon, \bar{\epsilon}]$, we have

$$g(\epsilon, \bar{\epsilon}) = \frac{1}{\bar{\epsilon} - \epsilon} \int_{\epsilon}^{\bar{\epsilon}} f(\eta) d\eta, \quad \epsilon = \epsilon^n = \epsilon(t_n), \quad \bar{\epsilon} = \epsilon^{n+1} = \epsilon(t_{n+1}). \tag{10}$$

The discretization in time is carried out with time step $\tau$, so that the scheme constructed has the following form

$$\begin{aligned}
&\frac{\epsilon_i^{n+1} - \epsilon_i^n}{\tau} = \frac{v_i^{\sigma_1} - v_{i-1}^{\sigma_1}}{h}, \quad i = 1, 2, \cdots, N-1, \\
&\rho \frac{v_i^{n+1} - v_i^n}{\tau} = \frac{s_{i+1}^{n+1} - s_i^{n+1}}{h}, \quad i = 0, 1, 2, \cdots, N-1, \\
&C_v \frac{\theta_i^{n+1} - \theta_i^n}{\tau} = k \frac{\theta_{i+1}^{\sigma_3} - 2\theta_i^{\sigma_3} + \theta_{i-1}^{\sigma_3}}{h^2} + k_1 \theta_i^{\sigma_3} \epsilon_i^{\sigma_2} \frac{v_i^{\sigma_1} - v_{i-1}^{\sigma_1}}{h}, i = 1, 2, \cdots, N-1, \\
&s_i^{n+1} = k_1(\theta_i^{\sigma_3} - \theta_1)\epsilon_i^{\sigma_2} - \frac{k_2}{4} g_1(\epsilon_i^n, \epsilon_i^{n+1}) + \frac{k_3}{6} g_2(\epsilon_i^n, \epsilon_i^{n+1}),
\end{aligned} \tag{11}$$

where

$$g_1(\epsilon, \bar{\epsilon}) = \frac{\bar{\epsilon}^4 - \epsilon^4}{\bar{\epsilon} - \epsilon} = \sum_{k=0}^{3} \bar{\epsilon}^{3-k} \epsilon^k, \quad g_2(\epsilon, \bar{\epsilon}) = \frac{\bar{\epsilon}^6 - \epsilon^6}{\bar{\epsilon} - \epsilon} = \sum_{k=0}^{5} \bar{\epsilon}^{5-k} \epsilon^k \tag{12}$$

and

$$y^{\sigma} = \sigma y^{n+1} + (1 - \sigma) y^n, \quad 0 \le \sigma \le 1. \tag{13}$$

The initial and boundary conditions are approximated as follows

$$\begin{aligned}
&\epsilon_i^0 = \frac{\partial u^0}{\partial x}(x_i), \quad v_i^0 = u^1(\bar{x}_i), \quad \theta_i^0 = \theta^0(x_i), \\
&s_0^{n+1} = \bar{s}_1(t_{n+1}), \quad s_N^{n+1} = \bar{s}_2(t_{n+1}). \\
&\frac{\theta_1^{\sigma_3} - \theta_0^{\sigma_3}}{h} - \frac{h}{2}\left(\frac{C_v}{k} \frac{\theta_0^{n+1} - \theta_0^n}{\tau} - \frac{k_0}{k} \theta_0^{\sigma_3} \epsilon_0^{\sigma_2} \frac{\epsilon_0^{n+1} - \epsilon_0^n}{\tau}\right) = \bar{\theta}_1^{\sigma_3} \\
&\frac{\theta_N^{\sigma_3} - \theta_{N-1}^{\sigma_3}}{h} + \frac{h}{2}\left(\frac{C_v}{k} \frac{\theta_N^{n+1} - \theta_N^n}{\tau} - \frac{k_0}{k} \theta_N^{\sigma_3} \epsilon_N^{\sigma_2} \frac{\epsilon_N^{n+1} - \epsilon_N^n}{\tau}\right) = \bar{\theta}_2^{\sigma_3}
\end{aligned} \tag{14}$$

Difference scheme (11)–(14) approximates the differential problem (11)–(14) with $O(h^2 + (\sigma_k - 0.5)\tau + \tau^2)$ order in space-time. In obtaining approximations (14) for the thermal field the standard technique of approximation of the third-kind boundary conditions with second order was applied (e.g., [10]).

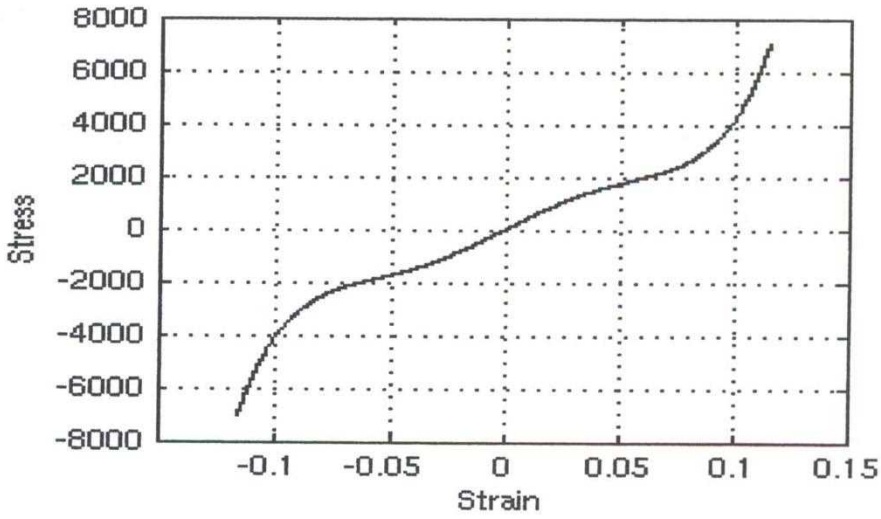


**Fig. 1.** Computed stress-strain dependency for the initial temperature $\theta^0 = 300°$ K.

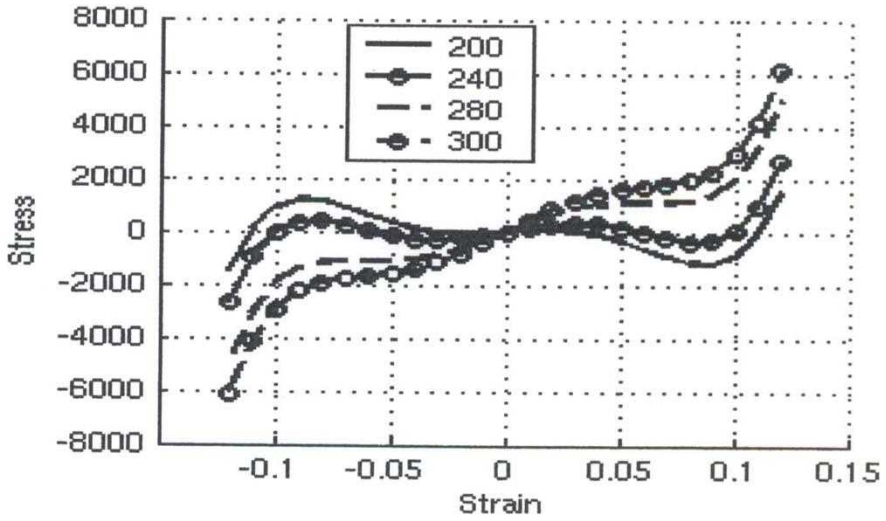


**Fig. 2.** A family of stress-strain curves computed with the algebraic equation.

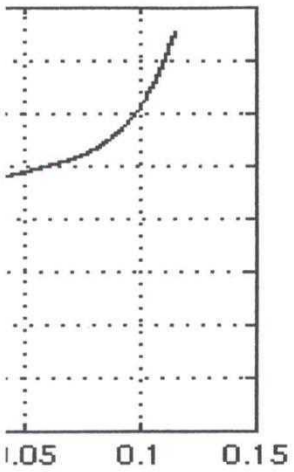


tial temperature $\theta^0 = 300°$

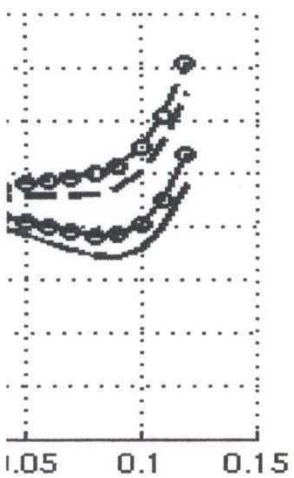


ith the algebraic equation.

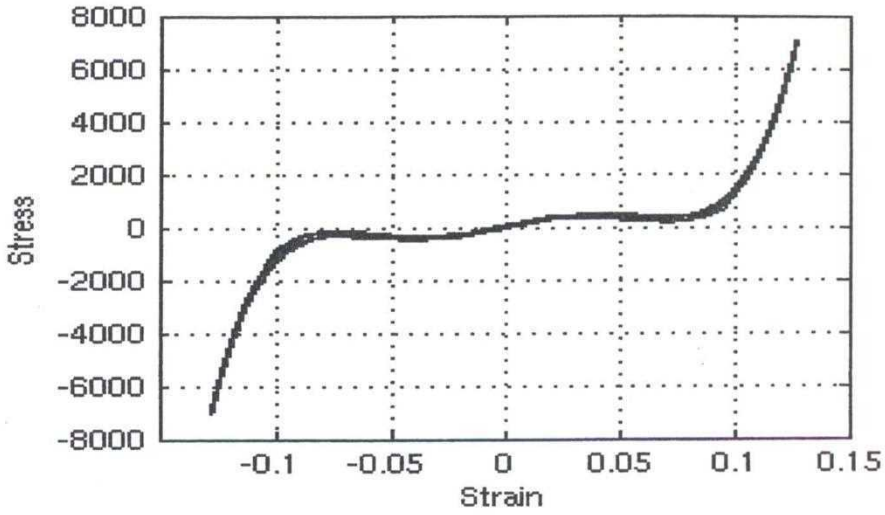


**Fig. 3.** Computed stress-strain dependency for the initial temperature $\theta^0 = 240°$ K.

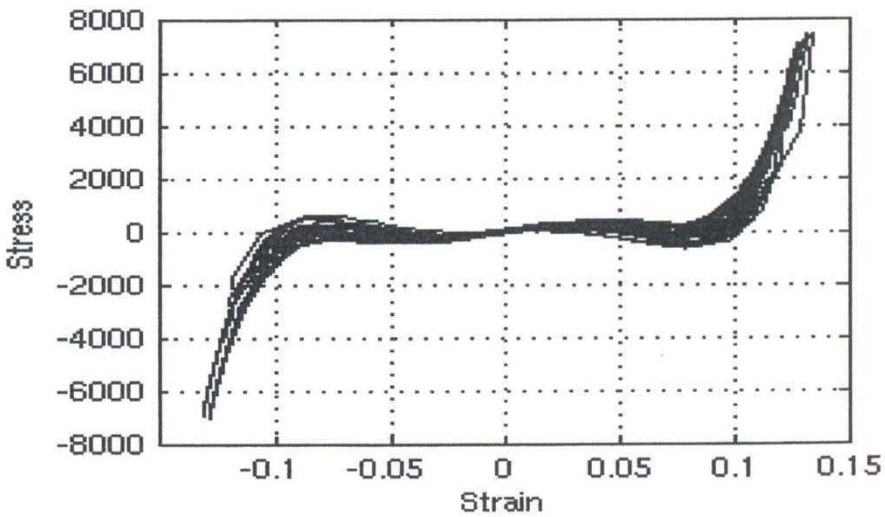


**Fig. 4.** Computed stress-strain dependency for the initial temperature $\theta^0 = 220°$ K.

## 4 Numerical Experiments

The scheme reported in Section 3 was applied to modelling the dynamics of a shape memory alloy rod under the stress boundary loading. Computational experiments reported here were performed for a $Au_{23}Cu_{30}Zn_{47}$ rod of length $L = 1$cm. For the $Au_{23}Cu_{30}Zn_{47}$ material all necessary parameters can be found in [2,3,5]. In the context of system (7), those physical constants are

$$k = 1.9 \times 10^{-2}\text{cmg/(ms}^3\text{K)}, \quad \rho = 11.1\text{g/cm}^3, \quad \theta_1 = 208\text{K},$$

$$k_1 = 480\text{g/(ms}^2\text{cmK)}, \quad k_2 = 6 \times 10^6\text{g/(ms}^2\text{cmK)},$$

$$C_v = 29\text{g/(ms}^2\text{cmK)}, \quad k_3 = 4.5 \times 10^8\text{g/(ms}^2\text{cmK)}.$$

In the discussion that follows all computations were performed for $N = 24$, and Newton's iterations with a Jacobian-based preconditioner were used for the solution of (10)–(14).

A Ginzburg capillarity effect is typically small for the Ginzburg coefficients reported in the literature. This effect has formally been included in the implementation, so that the condition of vanishing strain gradients on the boundary (e.g., [3,7])

$$\epsilon_x(0,t) = u_{xx}(0,t) = 0, \quad \epsilon_x(L,t) = u_{xx}(L,t) = 0 \tag{15}$$

has been assumed.

Let us consider first a situation where the initial thermomechanical conditions of the system are given as

$$\epsilon_i^0 = 0, \quad v_i^0 = 0, \quad \theta_i^0 = 300. \tag{16}$$

In other words, initially, the rod is in the austenitic phase which is stable under the given conditions. We assume no distributed thermomechanical forcing. We analyse the shape memory alloy dynamics during the first 42 ms, during which we apply a dynamically varying boundary stress according to the following rule

$$s(0,t) = s(1,t) = \begin{cases} -7000 sin^3(\frac{\pi t}{6}), & 0 < t \le 6, 24 < t \le 30, \\ 0 & 6 < t \le 12, 18 < t \le 24, 30 < t \le 36, \\ 7000 sin^3(\frac{\pi t}{6}) & 12 < t \le 18, 36 < t \le 42. \end{cases} \tag{17}$$

In Fig. 1 we present the computed stress-strain dependency. The figure demonstrates clearly that under the given thermomechanical conditions the rod behaves like an elastic material with weak nonlinearities. According to the classification given in [8], this is an almost-elastic behaviour where the free energy function, plotted as a function of strain, gives a well-defined single minimum that corresponds to our equilibrium configuration (austenite). In order to understand the situation better, in Fig. 2 we present a family of stress-strain characteristics obtained for different temperatures directly from the nonlinear equation for stress

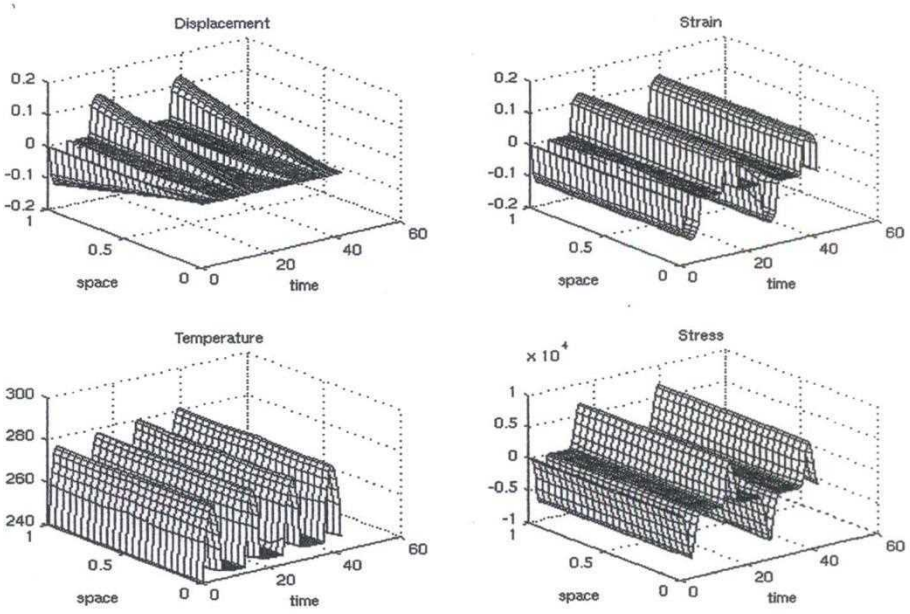


**Fig. 5.** Computed thermomechanical characteristics for problem (7), (16).

(see system (7)). It is clearly seen that if we decrease the temperature, nonlinearities in the stress-strain dependency would grow, reflecting the increasing importance of hysteresis effects. In Fig. 3 we present the computed stress-strain dependency for problem (7), (16) with initial condition for temperature taken as $\theta^0 = 240°K$. In this case, two emerging loops typical for the pseudoelastic behaviour are observed [8]. All three phases, one austenite and two (twin) martensites, may coexist, and the free energy function in this case contains three minima that correspond to these equilibrium configurations. Decreasing further the initial temperature would lead to a quasiplastic state. In particular, in Fig. 4 we present the computed stress-strain dependency for problem (7), (16) with the initial condition for temperature taken as $\theta^0 = 220°K$. In this case the stress-strain dependencies vary substantially over the temperature range of operation, exhibiting strongly nonlinear behaviour. The free energy function in this case has two well-pronounced minima that correspond to the martensitic twins. Finally, in Fig. 5 we present the dynamics of the rod under the conditions (16) in terms of displacement, temperature, strain and stress as functions of space and time.

## 5 Conclusions

In this paper we have presented a new conservative difference scheme which we have applied to the description of the thermomechanical dynamics of a shape memory alloy rod. One of the main properties of the proposed scheme is its

conservation of the total energy of the system on the grid, and in this sense the scheme is superior to other schemes previously proposed. The results of numerical simulations with this scheme have been reported here for the first time. They demonstrate that even on fairly coarse grids the scheme is capable of reproducing all main features of the dynamics of shape memory alloys, including hysteresis effects.

## References


1. Auricchio,F.,and Sacco,E.: Thermo-mechanical modelling of a superelastic shape memory wire under cyclic stretching-bending loadings. International Journal of Solid and Structure 38 (2001) 6123-6145
2. Falk,F.: Model free energy, mechanics, and thermomechanics of shape memory alloys. Acta Metallurgica 28 (1980) 1773-1780
3. Niezgodka,M., Sprekels,J.: Convergent numerical approximations of the thermomechanical phase transitions in shape memory alloys. Numer.Math. 58 (1991) 759-778
4. Melnik,R.V.N., Roberts,A.J., and Thomas,K.A.: Computing dynamics of copper-based SMA via centre manifold reduction of 3D models. Computational Materials Scinece 18 (2000) 255-268
5. Melnik,R.V.N., Roberts,A.J., and Thomas,K.A.: Coupled thermomechanical dynamics of phase transitions in shape memory alloys and related hysteresis phenomena. Mechanics Research Communications 18(6) (2001) 637-651
6. Bubner,N.: Landau-Ginzburg model for a deformation-driven experiment on shape memory alloys. Continuum. Mech. Thermodyn. 8 (1996) 293-308
7. Bubner,N., Mackin,G., and Rogers,R.C.: Rate dependence of hysteresis in one-dimensional phase transitions. Computational Material Science 18 (2000) 245-254
8. Melnik,R.V.N., Roberts,A.J., and Thomas,K.A.: Phase transitions in shape memory alloys with hyperbolic heat conduction and differential algebraic models. Computational Mechanics 29(1) (2002) 16-26
9. Matus,P., Melnik,R.V.N., and Rybak,I.V.: Fully Conservative Difference Schemes for Nonlinear Models Describing Dynamics of Materials with Shape Memory. Dokl. of the Academy of Sciences of Belarus 47 (2003) 15–18
10. Samarskii, A.A.: The Theory of Difference Schemes. Marcel Dekker, N.Y. (2001)
11. Abrashin, V.N.: A class of finite difference schemes for nonstationary nonlinear problems of mathematical physics. Differ. Equations 22 (1986) 759–769
12. Furihata, D.: A stable and conservative finite difference scheme for the Cahn-Hilliard equation. Numer. Math. 87 (2001) 675–699